

University of Nebraska - Lincoln

DigitalCommons@University of Nebraska - Lincoln

US Department of Energy Publications

U.S. Department of Energy

2001

Vibrational Structure and Vibronic Coupling in the Carbon 1s Photoelectron Spectra of Ethane and Deuteroethane

Tor Karlson
University of Bergen

Leif J. Sæthre
University of Bergen

Knut J. Børve
University of Bergen

Nora Berrah
Western Michigan University

Edwin Kukk
University of Oulu

See next page for additional authors

Follow this and additional works at: <https://digitalcommons.unl.edu/usdoepub>

 Part of the [Bioresource and Agricultural Engineering Commons](#)

Karlson, Tor; Sæthre, Leif J.; Børve, Knut J.; Berrah, Nora; Kukk, Edwin; Bozek, John D.; Carroll, Thomas X.; and Thomas, T. Darrah, "Vibrational Structure and Vibronic Coupling in the Carbon 1s Photoelectron Spectra of Ethane and Deuteroethane" (2001). *US Department of Energy Publications*. 36.
<https://digitalcommons.unl.edu/usdoepub/36>

This Article is brought to you for free and open access by the U.S. Department of Energy at DigitalCommons@University of Nebraska - Lincoln. It has been accepted for inclusion in US Department of Energy Publications by an authorized administrator of DigitalCommons@University of Nebraska - Lincoln.

Authors

Tor Karlson, Leif J. Sæthre, Knut J. Børve, Nora Berrah, Edwin Kukk, John D. Bozek, Thomas X. Carroll, and T. Darrah Thomas

Vibrational Structure and Vibronic Coupling in the Carbon 1s Photoelectron Spectra of Ethane and Deuteroethane

Tor Karlsen,^{*,†} Leif J. Sæthre,[†] Knut J. Børve,[†] Nora Berrah,[‡] Edwin Kukk,[§] John D. Bozek,^{||} Thomas X. Carroll,[⊥] and T. Darrah Thomas[#]

Department of Chemistry, University of Bergen, NO-5007 Bergen, Norway, Physics Department, Western Michigan University, Kalamazoo, Michigan 49008, Department of Physical Sciences, University of Oulu, FIN-90014 Oulu, Finland, Advanced Light Source, Lawrence Berkeley National Laboratory, University of California, Berkeley, California 94720, Keuka College, Keuka Park, New York 14478, and Department of Chemistry, Oregon State University, Corvallis, Oregon 97331-4003

Received: March 7, 2001; In Final Form: May 23, 2001

The carbon 1s photoelectron spectrum of ethane, C₂H₆, has been measured at a photon energy of 329 eV and an instrumental resolution of 70 meV. The spectrum shows a rich vibrational structure which is resolved using least-squares fits to the data. Only C–H stretching and CCH bending modes contribute significantly to the spectrum. The lack of excitation of the C–C stretching mode is explained in terms of changes in hybridization at the spectator carbon. To investigate the possibility of incomplete localization of the core hole, the spectra of C₂H₆ and C₂D₆ were measured at higher experimental resolution (35 meV). The spectra are accurately fit by a model based on ab initio calculations of the vibrational energies and the geometry changes following ionization, and including vibronic coupling of the two degenerate, localized hole states. A small splitting on the order of 10–20 meV is found for the ²A_{2u} and ²A_{1g} core-ionized states.

I. Introduction

Fine structures are important elements of high-resolution molecular X-ray photoelectron spectra, providing chemical information beyond that related to shifts in the ionization energy. First, vibrational structures reflect the properties of the energy surfaces of the neutral and core-ionized molecules, thus providing information about the nuclear and electronic dynamics of the ionization process. Second, molecular-field splitting of inner-shell p and d orbitals provides insight into the asymmetry of the surroundings of the center of ionization. Finally, core orbitals on neighboring atoms of the same element may interact, leading to delocalized core orbitals. Inner-shell ionization then leads to finely split core-hole states, which may couple via one or several vibrational modes—a situation referred to as vibronic coupling. The resulting photoelectron spectrum shows characteristics both of the difference in ionization energy due to the bonding–antibonding interaction and of the vibronic coupling, most notably in the adiabatic peaks, but also in the vibrational structure.

For carbon 1s photoelectron spectra of hydrocarbons, we are concerned with vibrational excitation and, in some cases, vibronic coupling. Methane has a well-understood vibrational structure where only one vibrational mode, the symmetric C–H stretching mode, is Franck–Condon (FC) active. Vibronic coupling is not important in methane since there is only one carbon in the molecule. Replacing one of the hydrogens in methane with a methyl group gives ethane, a prototype molecule for the saturated linear hydrocarbons. The spectrum of ethane

shows rich vibrational structure, and an understanding of the change in geometry that follows ionization is imperative for an accurate description of the spectrum. In addition, since ethane contains two equivalent carbon atoms, it is also necessary to consider vibronic coupling.

Several high-resolution studies of the carbon 1s photoelectron spectrum of ethane have been reported.^{1–6} To summarize, only two vibrational modes are significantly excited. One is a C–H stretching mode, ν_1 , with a fundamental vibrational energy of 398–407 meV, and the other is a CCH bending mode, ν_2 , with a fundamental frequency of 176–185 meV. The C–C stretching mode has the right symmetry to be Franck–Condon active, but none of the previous studies have found experimental evidence for excitation of this mode, although Osborne et al.⁵ mistook the shoulder at the main peak as evidence for excitation of this mode. Rennie and co-workers³ assured an unambiguous assignment by measuring the isotopic shifts in vibrational energies. So qualitatively, the vibrational structures are rather well understood.

Core ionization leads to a high degree of excitation of the C–H stretching mode, indicating a contraction of the valence shell of the core-ionized carbon. In light of this, it is puzzling that the C–C stretching mode is hardly excited. A justification of the geometry changes following the excitation is therefore in order.

Recently we showed that the use of an effective core potential, ECP, in electronic structure calculations for carbon 1s ionized molecules gives accurate estimates of the change in geometry upon core ionization of methane.⁷ An ECP represents a localized core hole, and in the case of ethane such a model assumes the vibrational motion to follow the diabatic energy surface. The accuracy of this approximation can be estimated from the electronic coupling integral, β , between the two degenerate states featuring the core hole localized at either of the two carbon

* Author to whom correspondence should be addressed.

† University of Bergen.

‡ Western Michigan University.

§ University of Oulu.

|| Lawrence Berkeley National Laboratory, University of California.

⊥ Keuka College.

Oregon State University.

atoms. Previous studies have shown that the vibrational structures in the carbon 1s spectrum of ethane are well represented by a localized core-hole model,^{5,6} suggesting a small value of β .

In this work, the high-resolution C1s photoelectron spectra of C₂H₆ and C₂D₆ have been recorded using third-generation synchrotron radiation, which makes it possible to obtain spectra with higher resolution and intensity than has previously been available. Fitting the peaks in the spectrum by least squares gives the vibrational energies and intensities of the significant transitions as well as information on the anharmonicity of vibrational modes, which have been found to be significant in the case of methane.⁷ A second fit, based on ab initio calculations at the MP2 level of theory provides a test of the theoretical predictions. These calculations are based on the ECP core-hole model, which goes beyond the much-used equivalent-cores approximation. They also use data on the anharmonicity for methane in the calculation of Franck–Condon factors. This procedure constitutes a validation of a rather simple theoretical procedure for analyzing inner-shell photoelectron spectra of saturated linear hydrocarbons. Next, the diabatic localized core-hole model is investigated both theoretically and experimentally. Finally, we rationalize the change in equilibrium geometry that accompanies the ionization of an inner-shell electron in ethane by considering how hybridization of carbon changes as a response to the ionization.

II. Experimental Procedure

Carbon 1s photoelectron spectra were acquired at beamline 10.0.1 at the Advanced Light Source (ALS) of Lawrence Berkeley National Laboratory. The measurements were made using a photon energy of 329 eV. This is about 38 eV above the ionization threshold, and the interaction between electrons from the Auger decay process and the photoelectron (post-collision interaction, or PCI) is relatively small. The spectrometer was aligned at an angle of 54.7° to the electric-field vector of the light and at 90° to the propagation direction of the beam. Beamline 10.0.1 receives its radiation from a 10-cm-period undulator (U10) and a spherical grating monochromator that is capable of a resolving power ($E/\Delta E$) of about 10⁴. The kinetic energy of the photoelectrons was analyzed using a Scienta SES-200 hemispherical electron energy analyzer.⁸

The first set of measurements was performed before beamline 10.0.1 had all facilities in operation (August 1998), and a total analysis of the different contributions to the instrumental resolution was not possible. From argon 2p photoemission measurements, the total instrumental resolution was estimated to 70 meV (full width at half-maximum, or fwhm) and Gaussian in shape. To gain insight into the splitting between the ²A_{1g} and ²A_{2u} core-hole states, a second set of measurements was made in November 2000 at the same photon energy and with settings optimized to get as high resolution as possible. Spectra for both C₂H₆ and C₂D₆ were recorded with the same experimental settings. The energy analyzer was characterized using the xenon 5s photoelectron line with negligible contributions from the intrinsic width and the photon bandwidth. By choosing a kinetic energy similar to that of the carbon 1s photoelectrons, the properties of the analyzer were obtained under the appropriate conditions. The total instrumental broadening, including the Doppler effect, was determined to 35 meV (fwhm).

Ethane (99.97%) was obtained from Matheson and *d*₆-ethane (98%) from Cambridge Isotope Laboratories, Inc. The gases were introduced into the inlet system without further purification. Data acquisition was made in a series of short runs,

with the data from each run being inspected and the energy scale adjusted to account for small drifts in energy. Since neither the photon energy nor the absolute electron kinetic energy are accurately known, the ionization-energy scales are shifted so that the peak corresponding to adiabatic ionization is at 290.55 eV for C₂H₆⁹ and 290.52 eV for C₂D₆.¹⁰

III. Theoretical Aspects

A. Vibronic Coupling Theory. A theoretical account of vibronic coupling in core-ionized ethyne is given elsewhere.¹¹ Here we review the essential features of this approach and expand it to cover molecules in which several vibrational modes may contribute to localize the core hole.

The theoretical treatment starts from a basis with the core hole localized on one or the other of the equivalent carbon atoms: $\Psi_L = |\Phi_L\rangle|\nu_L\rangle$ and $\Psi_R = |\Phi_R\rangle|\nu_R\rangle$. Here, $|\Phi\rangle$ indicates an electronic function for an ion with the core hole localized either on the left or the right carbon atom, and $|\nu\rangle$ refers to a vibrational function appropriate to an ion with a localized hole. In the analysis of ethyne, only one vibrational mode was considered. In the more general case, considered here, ν is a vector indicating the quantum numbers of all of the vibrational modes.

The Hamiltonian of the system includes both electronic and nuclear terms: $\hat{H} = \hat{T}_N + \hat{H}_e$. At the level of first-order degenerate perturbation theory, the vibronic energy levels are

$$E = \epsilon_\nu \pm \beta \langle \nu_L | \nu_R \rangle \quad (1)$$

where ϵ_ν designates a vibrational energy of the ion with a localized hole, and β is the electronic coupling integral, $\langle \Phi_L | \hat{H}_e | \Phi_R \rangle$. Thus, each vibrational level is split by the electronic interaction by $2\beta \langle \nu_L | \nu_R \rangle$. Since the overlap integral depends on the particular vibrational state, this splitting can vary from one vibrational state to another. At this level of approximation, the vibrational intensities are given by the Franck–Condon factors appropriate to an ion with a localized hole.

In the limit that the second term of eq 1 is negligibly small, the vibrational spectrum observed in core-ionization is simply that for an ion with a localized hole. Such a model has been successfully used to interpret spectra for a number of systems in which β is expected to be very small. At the other extreme, if there is need to go beyond the first-order treatment, both energies and intensities will be affected, as is the case for ethyne.

Within the framework of this model, there are several steps involved in making a theoretical prediction of the vibronic spectrum. (1) Calculate the optimized geometries, electronic wave functions, and vibrational frequencies for the neutral and core-ionized molecules. (2) Calculate the Franck–Condon intensities for excitation of the vibrational states for an ion with a localized core hole. (3) Calculate β from the electronic wave functions and calculate the vibrational overlap integrals $\langle \nu_L | \nu_R \rangle$. Then eq 1 gives the first-order result for the energies. If it is necessary to go beyond first-order, then two more steps are necessary. (4) Calculate the off-diagonal matrix elements, $\pm \beta \langle \nu_L | \nu_R \rangle$, and diagonalize the resulting matrix to give the energy levels. (5) From the eigenvectors of this matrix and the Franck–Condon factors calculate the intensity for each vibrational level.

For ethane β is expected to be small but not negligible and we anticipate that only the first three steps are necessary. Some of these steps present their own set of problems, which we discuss in more detail below.

B. Electronic Structure Calculations. Much of the earlier work done on vibrational structures in XPS spectra was based

on the equivalent-cores approximation where, in the case of inner-shell ionization of carbon, C^* is replaced by the isovalent N^+ . Generally, the equivalent-cores approach was found to overestimate the C–H bond shrinkage considerably, although this may to a large extent be remedied by replacing the nitrogen basis set with a restricted carbon basis.⁶ However, such an approach is conceptually unsatisfying since it is not possible to systematically improve the accuracy of a calculation by increasing the one- and N -particle bases. In the present approach of representing the ionized core by an effective core potential, we retain the computational simplicity of the equivalent-cores model, but gain flexibility in the choice of basis sets (e.g., ref 7).

The details of the electronic structure calculations are given in the appendix, and only the main features are outlined here. Equilibrium geometries, harmonic vibrational frequencies, and normal-mode vectors were calculated using second-order perturbation theory as formulated by Møller and Plesset (MP2)¹² using the Gaussian 94 package.¹³ All calculations were done with ethane in a staggered geometry, leading to D_{3d} symmetry for the ground state and C_{3v} symmetry for the ion with a localized core hole. From the electronic wave functions, the value of the electronic coupling integral, β , is calculated to be 11.5 meV.

The harmonic frequencies obtained by this procedure are expected to be higher than the observed frequencies. As an empirical correction for this failure, we use the known frequencies for the ground-state molecule,¹⁴ and scale the frequencies for the ionic state by the ratios of observed-to-calculated frequencies for the neutral state. The scaling factors are 0.98 for C–C stretching and 0.94 to 0.96 for modes involving hydrogen motion.

C. Franck–Condon Amplitudes. While it is straightforward to calculate vibrational overlap integrals for a diatomic molecule, in polyatomic molecules the normal modes of the ground state do not necessarily coincide with those of the core-ionized state. For instance, in the ground state of ethane the C–H stretching and CCH bending motion are coupled to symmetric and antisymmetric modes, whereas in the core-ionized molecule with a localized hole these become local C–H stretching and CCH bending modes. This problem can be dealt with using procedures such as that given by Malmqvist and Forsberg,¹⁵ and we have used their approach here to calculate relative vibrational intensities for an ion with a localized core hole. As it turns out, the procedure that we have used earlier, based on an approximate one-to-one mapping between ground and final state normal modes,⁶ leads to an intensity distribution essentially identical to that of the more complete theory. The reason is that ionization primarily leads to rotation of normal modes that are close to degenerate, and the vibrational profile is little influenced by redistribution of intensity between closely spaced lines. However, we have found it necessary to compute the left–right overlap integrals $\langle \nu_L | \nu_R \rangle$ appearing in eq 1 by means of the full procedure.¹⁵

The calculated Franck–Condon intensities are extremely sensitive to changes in bond lengths and bond angles. At the level of theory used here, the bond shrinkage upon core ionization is exaggerated by 0.2 pm in methane. To account for this, the optimized C–H bond length in the core-ionized CH_3 group in ethane has been adjusted accordingly.

IV. Models Used To Fit the Vibrational Structure

The photoelectron spectrum has been fit using two different procedures, to be denoted *free fit* and *theoretical fit*, respectively.

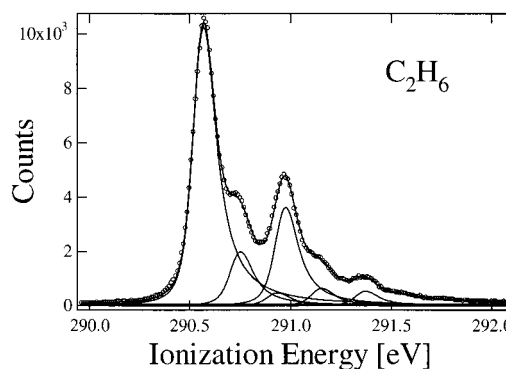


Figure 1. Carbon 1s photoelectron spectrum of ethane, as given by the circles, with an experimental resolution and lifetime broadening of 70 and 100 meV (fwhm), respectively. The solid line represents a free fit to the spectrum, as described in the text.

TABLE 1: Vibrational Energies and Relative Intensities for the C–H Stretching (ν_1) and CCH Bending (ν_2) Modes in Ethane upon Ionization of C1s As Obtained from a Free Fit of 9 Peaks to the Spectrum in Figure 1^a

$\nu_1 \nu_2^b$	energy (meV)	relative intensity
0 0	0.0	1.0
0 1	182.8 (1.4)	0.193 (0.004)
0 2	365 (24)	0.047 (0.049)
1 0	404.9 (2.9)	0.361 (0.050)
1 1	584.5 (2.2)	0.064 (0.002)
1 2	746 (33)	0.007 (0.007)
2 0	802 (5)	0.052 (0.006)
2 1	992 (8)	0.008 (0.002)
3 0	1179 (19)	0.001 (0.001)

^a Statistical uncertainties are shown within parentheses. ^b Vibrational quantum numbers for the C–H stretching and the CCH bending modes.

In the free fit, a set of peak positions and intensities were determined by least-squares techniques.¹⁶ In the theoretical fit, the energy spacing and relative intensities of vibrational lines were obtained from ab initio calculations, and the only fitting parameters were constant background, overall intensity, and overall position. In both the free and theoretical fit, a line shape including instrumental resolution, lifetime broadening, and post-collision interaction (PCI) was used, with a Lorentzian lifetime width of 100 meV. Gaussian widths of 70 meV for the free fit and 35 meV for the theoretical fit were used for the instrumental resolution. The PCI effect is included by the approach given by van der Straten et al.¹⁷

In principle, there are five vibrational modes that might contribute to the spectrum in the Franck–Condon approximation. Previous analyses^{1–3,5} indicate that only two of these modes contribute significantly, of which the more important is a carbon–hydrogen stretch, ν_1 . A peak corresponding to the fundamental excitation of this mode is apparent in Figure 1, at an ionization energy of about 0.4 eV above the principal peak. The other important mode, seen as a shoulder on the main peak, describes a CCH bending motion (ν_2) with fundamental frequency of about 0.18 eV. The most accurate theoretical calculations presented later in the paper indicate a minute excitation of the CC stretching mode (ν_3), and in light of this, we have restricted our free fit to only two modes. In the free fit, we have included nine peaks as represented by their quantum numbers given in Table 1; the nineteen free parameters are background, absolute intensity, and position of the main peak, and the intensities and positions of the remaining eight peaks relative to the main peak.

In the theoretical fits vibrational energies and Franck–Condon (FC) intensities were taken from calculations. Vibrational

energies and intensities were computed within the harmonic oscillator approximation, except as detailed below, and vibrational states receiving a relative intensity larger than 0.001 were included in the fits.

The theoretical treatment represents a compromise between feasibility and completeness, and suffers from several shortcomings. A harmonic model often leads to predicted vibrational energies that are too large because of the neglect of anharmonicity. The anharmonicity will also affect the intensity, and the actual intensities of higher excited states are usually lower than what is predicted using a harmonic model. Detailed analyses of the vibrational structures in the carbon 1s photoelectron spectrum of methane have shown that the symmetric C–H stretching mode in methane is significantly anharmonic, and better described as a Morse oscillator.¹⁸ Here, the localized C–H stretching coordinates in ethane are described in terms of Morse potentials, with parameters taken from the methane isotopomers, for both neutral¹⁹ and core-ionized states.²⁰

V. Results

We have measured two sets of spectra, one with an experimental resolution of 70 meV and the other with 35 meV. The first has very good statistics and is well suited for accurate determination of energies and intensities, especially with respect to the low intensity peaks. This spectrum is used in the *free fit* and in the investigation of possible anharmonicity. The higher resolution spectra of C₂H₆ and C₂D₆ are used to gain insight in the possible splitting of the ²A_{1g} and ²A_{2u} states; the narrower lines shapes allow for an evaluation of the accuracy of the theoretical procedure.

The spectrum of C₂H₆ at 70-meV resolution is presented in Figure 1 where experimental data are given by circles while the solid line represents the free fit to the spectrum. The fit has a reduced value of χ^2 (goodness-of-fit) of 1.88. Values of the resulting energies and intensities are listed in Table 1. The uncertainties, shown in parentheses in Table 1, are the standard deviations calculated by the least-squares routine from the inverse of the curvature matrix.²¹ Inspection of Table 1 shows that the fundamental vibrational frequency for the C–H stretching mode is 404.9 ± 2.9 meV and that for the CCH bending mode is 182.8 ± 1.4 meV.

From the intensities and energies in Table 1, we obtain the average vibrational excitation energy of core-ionized ethane to be 169 meV. Assuming that this value is independent of the photon energy and subtracting it from the vertical ionization energy reported by Sæthre et al.²² of 290.70 ± 0.05 eV, we obtain an adiabatic ionization energy of 290.53 eV. This is in excellent agreement with the recent value of 290.55 eV obtained by Myrseth et al.,⁹ but significantly different from the value of 290.42 eV suggested by Osborne and co-workers.⁵ The latter result was based on an estimate of 0.28 eV for the average vibrational energy; this is, however, not supported by the energies and intensities given by them, which lead to a value of only 0.19 eV, close to our value. The referenced ionization energies were obtained in XPS measurements using conventional²² and synchrotron^{5,9} radiation sources, and differ mainly in energy resolution and description of the vibrational structure.

Including only two vibrational modes, the vibrational energies are given according to second-order perturbation theory by

$$E_{vib}(v_1, v_2) = \sum_{i=1}^2 \left(v_i + \frac{1}{2} \right) \omega_i + \sum_{i \geq j}^2 \left(v_i + \frac{1}{2} \right) \left(v_j + \frac{1}{2} \right) X_{ij} \quad (2)$$

where ω_1 and ω_2 represent harmonic frequencies and X_{11} , X_{12} ,

TABLE 2: Spectroscopic Constants (meV) for Core-Ionized Ethane As Obtained Using Eq 2 in a Least-Squares Fit to the Spectrum Shown in Figure 1^a

	H ₃ C*CH ₃ ⁺
ω_1	407.2 (2.0)
ω_2	184.5 (2.2)
X_{11}	-1.6 (1.1)
X_{12}	-0.5 (1.6)
X_{22}^b	0

^a Statistical uncertainties are shown within parentheses. ^b X_{22} was not allowed to change in the fit.

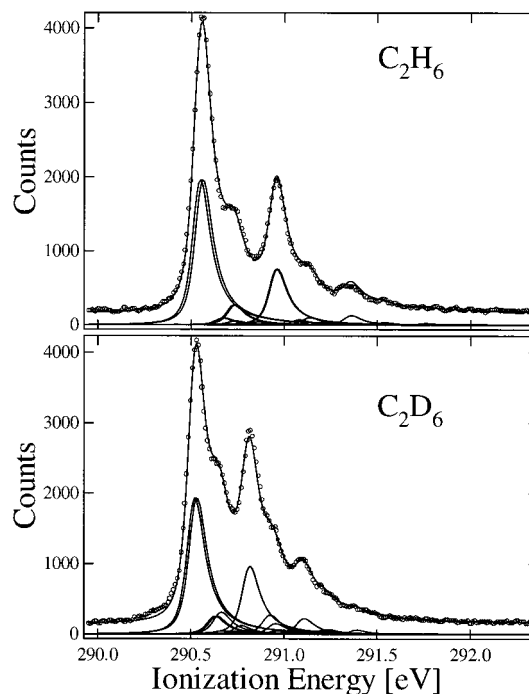


Figure 2. Theoretical fits (solid line) to the carbon 1s photoelectron spectra (circles) of C₂H₆ and C₂D₆, with instrumental resolution of 35 meV and lifetime width of 100 meV (fwhm).

and X_{22} are second-order anharmonic constants. The subscripts 1 and 2 refer to the C–H stretching and CCH bending modes, respectively. The spectroscopic constants reported in Table 2 are obtained by using eq 2 as a model in a least-squares fit to the spectrum of ethane, as presented in Figure 1. Because of the low statistical significance of the (0,2) peak, X_{22} was fixed at zero in the fitting procedure. The anharmonicity constant for the stretching mode, X_{11} , is significant and given by -1.6 ± 1.1 meV, close to the value of -1.9 meV found for methane.²⁰ The magnitudes of X_{11} and X_{12} are close to their corresponding statistical uncertainties. Use of eq 2 reduces the number of energy parameters in the fitting procedure from 9 to 6 as compared to the free fit. Such a procedure gives improved energies as compared to the linear-coupling model used in some of the previous studies.^{2,3,5} The linear-coupling model assumes equidistant energies and fails in the case of significant anharmonicity.

Our theoretical fits to the spectra of C₂H₆ and C₂D₆ at 35-meV resolution are shown in Figure 2. The calculated effects of vibronic coupling of the ²A_{2u} and ²A_{1g} core-ionized states (see below) are included in the fits. Only the main peak is noticeably affected by the coupling, with a calculated splitting of 14 and 11 meV, respectively, for C₂H₆ and C₂D₆. The splitting of the excited vibrational states is very small. The reduced values of χ^2 for the fits are 1.46 and 2.03 for C₂H₆ and C₂D₆, respectively. The lower quality of the fit to the C₂D₆ spectrum

TABLE 3: Calculated Vibrational Energies and Relative Intensities for the C–H Stretching (ν_1) and CCH Bending (ν_2) Modes in Core-Ionized Ethane

$\nu_1 \nu_2^a$	C_2H_6		C_2D_6	
	energy (meV)	rel. intensity	energy (meV)	rel. intensity
0 0	0.0	1.0	0.0	1.0
0 1	179.5	0.161	137.5	0.182
0 2	359.2	0.018	274.5	0.020
1 0	404.9	0.386	291.9	0.502
1 1	584.6	0.062	429.7	0.091
1 2	763.6	0.006	566.6	0.010
2 0	806.5	0.066	582.1	0.117
2 1	986.0	0.011	719.9	0.021
3 0	1204.0	0.006	870.7	0.016

^a Vibrational quantum numbers of the C–H stretching and CCH bending mode, where ν_1 and ν_2 describe excitations levels of the two C–H stretching and the two CCH bending modes, respectively (see Results for details).

just below threshold is probably due to the gas not being 100% pure. Except for the splitting of the main peak, the qualitative results are essentially the same as those given by Thomas et al.⁶ The symmetric and antisymmetric C–H stretching and CCH bending modes in neutral ethane are combined in core-ionized ethane to give stretching and bending modes that are mostly localized to one carbon center. For the two CCH bending modes the localization is not complete and both modes are excited. The shoulder on the adiabatic peak is an 83%–17% distribution of excitation of the two bending modes, leading to a minor broadening as compared to representing the shoulder by a single peak as in the free fit. Thus, according to the calculations, the vibrational progression of ν_2 is a progression of two bending modes, and the features appearing in the spectrum will be a weighted average of the underlying lines. The theoretical calculations also predict slight excitation of the C–H stretching mode on the spectator carbon, and the corresponding intensities will contribute to the part categorized as the ν_1 progression. Average energies and intensities for ν_1 and ν_2 for C_2H_6 and C_2D_6 are listed in Table 3. The major vibrational progression arises from the C–H (C–D) stretching mode, with a weighted average frequency of 405 (292) meV for C_2H_6 (C_2D_6). Second in importance is a CCH (CCD) bending mode with a calculated frequency of 180 (137) meV, mainly involving hydrogen atoms attached to the spectator carbon. The fundamental frequency for the CC stretching mode, ν_3 , was computed to be 121 (107) meV, and with an intensity of 0.049 (0.13) for the $\nu_3 = 1$ line.

VI. Discussion

A. Vibrational Modes and Their Energies. From the free-fit procedure, we obtain energies of 404.9 ± 2.9 meV for the C–H stretching mode and 182.8 ± 1.4 meV for the CCH bending mode. The uncertainties are most likely larger than the statistical uncertainties indicated here and listed in Table 1, because of the assumption of only two excited vibrational modes, neglect of factors such as Fermi resonance, vibronic coupling, and nonperfect line shapes. Previously reported values range from 398 to 407 meV for the stretching mode and from 176 to 189 meV for the bending mode,^{1–3,5} bracketing our values. The value of χ^2 for the fit (1.88) indicates that there are small discrepancies remaining between the model and the data. A part of these may arise from our assumptions about the line shape. Analysis of the photoelectron spectrum of methane shows that there are systematic differences between predictions based on the present PCI model and the observed spectrum,¹⁸ especially close to threshold.

For the C–H stretching mode, the ab initio MP2 model gives a weighted-average fundamental frequency of 405 meV, in excellent agreement with the value of 404.9 ± 2.9 meV from the free fit. Furthermore, the model leads to an energy of 180 meV for the CCH bending mode, close to 182.8 ± 1.4 meV from the free fit. The average vibrational energy from the MP2 calculations is 184 meV, about 9% higher than the value of 169 meV from the free fit. The difference is mainly given by the overestimation of the intensities corresponding to higher vibrational quantum numbers using the harmonic oscillator approximation.

B. Effects of Vibronic Coupling. In the theoretical calculations, we have used a model for the core-ionized state where the core hole is localized to one of the carbon atoms. Using a localized core-hole description of the ion is equivalent to what is known as the diabatic approximation. A detailed theoretical analysis of the diabatic approximation has recently been given for ethyne.¹¹ Following ref 11, the true vibronic states may be expressed in terms of localized-hole electronic wave functions multiplied by their vibrational counterparts, i.e., in a diabatic basis. Since these electronic wave functions change only slowly with the nuclear coordinates, coupling between the diabatic states occurs mainly through the electronic Hamiltonian. Hence, the accuracy of the diabatic approximation, i.e., when the electronic coupling is neglected, may be assessed by the magnitude of the electronic coupling integral, multiplied by a vibrational overlap integral, cf. eq 1. Taking into account that the diabatic states are slightly nonorthogonal, the electronic coupling integral β is given by $\beta = H_{LR} - S_{LR} (H_{LL} + H_{RR})/2$, where S and H denote electronic overlap and energy integrals for states having the core hole localized on the left and right carbon. An upper bound to the separation of the ${}^2A_{1g}$ and ${}^2A_{2u}$ states is 2β , which is computed to be 23 meV, as detailed in the Appendix. This number agrees well with the difference of 17 meV between orbital energies of $1a_{1g}$ and $1a_{2u}$ orbitals in neutral ethane. Neutral-molecule orbital energies were also found to give a reasonable estimate of 2β in the case of ethyne.²³ Calculated values of the $\langle \nu_L = 0 | \nu_R = 0 \rangle$ overlap integrals in conjunction with eq 1, give splittings of 14 and 11 meV for the $\nu = 0$ states of core-ionized C_2H_6 and C_2D_6 , respectively.

The splitting of the $\nu = 0$ levels of the ${}^2A_{1g}$ and ${}^2A_{2u}$ states may also be deduced experimentally by replacing the principal peak with two equivalent peaks (assuming equal cross sections for the two ionization channels) separated in energy by an adjustable parameter equal to this splitting. An accurate estimate of the splitting demands high resolution and a well-defined line shape. The C_2H_6 spectrum with experimental settings tuned for maximum resolution (35 meV) was therefore used for this purpose. Increasing the resolution reduces the intensity, but this is of less concern with respect to the main peak. The spectrum was then fit using the free-fit model with an additional (0,0) line, and with the Gaussian part of the width set to 35 meV. This procedure gives a value of 18 ± 3 meV for the splitting and 100 ± 2 meV for the Lorentzian contribution to the width.

A splitting of 18 ± 3 meV is in accord with the calculated value 14 meV. Although a splitting of some 10–20 meV is too small to be apparent in the present data, it would certainly affect a fit of the line shape and a comment about the extraction of lifetimes from spectra including close-lying states is in order. According to simple tests, a small splitting is mainly modeled by a broadening of the Gaussian component, while the Lorentzian part, representing the lifetime broadening, is hardly affected. This conclusion supports the credibility of the recent proposed value of 98 ± 10 meV for the lifetime broadening in ethane

TABLE 4: Internal Coordinates for the Equilibrium Geometry of C₂H₆ As Obtained from Experiment and Theory^a

internal coordinate	expt ^b	MCPF	MP2
R (C–C)	1.5351	1.5287	1.5243
R (C–H)	1.0940	1.0879	1.0857
A (CCH)	111.17	111.14	111.16

^a Bond lengths and angles are given in Ångström and degrees, respectively. ^b Reference 34.

TABLE 5: Geometry Changes Following Core-Ionization of C₂H₆ As Obtained from Experiment and Theory^a

internal coordinate ^b	expt ^c	MCPF	MP2
R (C*–C)		–0.41	–1.09
R (C*–H)	–5.1	–5.38	–5.46
R (CH)		–0.58	–0.46
A (C*CH)	–3.0	–2.89	–2.71
A (CC*H)		+0.03	+0.06

^a Bond lengths and angles are given in pm and degrees, respectively. ^b C* denotes the core-ionized carbon. ^c Reference 3.

based on a least-squares fit of a single set of peaks.³ A lifetime broadening of 98 meV is also in good agreement with our value of 100 ± 2 meV obtained when convoluting the adiabatic peak by two identical peaks.

C. Geometric Changes upon Core Ionization. In several previous studies,^{1–6} the main geometric changes accompanying core ionization have been identified. Using a localized core-hole model, Rennie et al.³ estimated the change in C*–H bond length to be -5.1 pm and the change in C*CH angle to -3.0° . They used a linear-coupling model, assuming harmonic frequencies common for both the neutral and the core-ionized molecule. However, in the case of significant anharmonicity, these assumptions may lead to errors in the order of tenths of a picometer.¹⁸

To validate the MP2 geometries, a set of highly accurate equilibrium geometries was computed. In these calculations the localized core hole was explicitly included and variationally optimized, and all valence electrons were correlated at a configuration–interaction level of theory (MCPF). Such high-level calculations are feasible only for small molecular systems and are useful for calibration purposes. Molecular geometries and geometry changes following ionization as obtained from experiments and as calculated at the MP2 and MCPF levels of theory are listed in Tables 4 and 5 (see Appendix for details of the calculations). Generally, MP2 performs very well for the geometry changes; the most pronounced difference as compared to MCPF being that the shortening of the C–C bond distance is more than doubled. In general, the more elaborate calculations reduce the shortcomings of the theoretical fit. If the MCPF result of 5.38 pm for the C–H bond contraction is lowered by the known overestimation of the C–H contraction from methane (0.15 pm),⁷ this gives a “best” estimate of the C–H contraction of 5.2 pm. The changes in geometry obtained from the MCPF calculations are in excellent agreement with the experimentally derived results of Rennie et al.³

The very small change in carbon–carbon distance (1 pm or less) is surprising in light of the appreciable change taking place for the C*–H bonds and the large C–C bond shrinkage in ethyne (4.4 pm).¹¹ Removal of a core electron leads to a reduced shielding of the valence electrons and a contraction of the electron density toward the nucleus at the core-hole site. This would be expected to reduce both the C*–C and the C*–H distances, and since this is not what is observed, there must be competing effects that counteract the C*–C bond reduction.

This is apparently absent in ethyne, for which the C–C bond shortens significantly upon ionization. To rationalize these geometry effects we turn to a simple hybridization model. The hybridization of the carbons has been obtained by a natural bond orbital (NBO) analysis,²⁴ giving orbitals localized to the different bonds and with bond-specific hybridization. The main results are as follows: For the C*–C bond, the hybridization of the spectator carbon changes from $sp^{2.4}$ to $sp^{3.3}$ upon ionization, a result that may be understood with reference to a “rule” formulated by Walsh in 1947:²⁵ *If a group X (read: CH₃) attached to carbon is replaced by a more electronegative group Y (read: C*H₃⁺), then the carbon valency toward Y has more p character than it has toward X.* Because of its directional character, increasing the C 2p contribution in the C–C* bond counteracts the effect of the more contracted valence at C*, leading to only a minute shortening of the bond.

In the case of acetylene, two of the three p orbitals at the carbon atoms are allocated to π bonds, leaving only carbon sp^1 hybrids for the C–C and C–H σ bonds. This limits the ability to increase the p character of the hybrid toward the core-ionized carbon; whereas Δn for the carbon hybrid directed toward the core-ionized carbon is 0.9 in the case of ethane, it is only 0.3 for C₂H₂. The behavior of Δn can justify the rather large difference in carbon–carbon bond contraction going from C₂H₂ to C₂H₆. This effect is obvious in the photoelectron spectra, where excitation of CC stretching is a major component of the spectrum for ethyne¹¹ but an insignificant component in ethane.

The computed change in C hybridization in ethane also provides an explanation for the change in C*CH angle, and for the sign of the change of the spectator C–H bond length. The spectator hybrids participating in the C–H bonds changes from $sp^{3.3}$ to $sp^{2.8}$. The C sp^n hybridization of the C–H bonds is related to the angle α between the bonds by $\cos(\alpha) = -1/n$.²⁶ The computed value of -0.5 for Δn corresponds to a decrease in C*CH angle of about 2.6° , in keeping with the value of -2.9° from the MCPF calculations. The small decrease (-0.5 pm) in C–H bond lengths is in the direction expected for this change in hybridization.

VII. Conclusions

The carbon 1s photoelectron spectrum of ethane has a rich vibrational structure dominated by two vibrational progressions, which correspond to excitation of a CCH bending mode ($\nu_2 = 182.8 \pm 1.4$ meV) and a C–H stretching mode ($\nu_2 = 404.9 \pm 2.9$ meV). For the C*–H stretching mode, an anharmonic constant, X_{11} , of -1.6 ± 1.1 meV was obtained. The ²A_{1g} and ²A_{2u} core-hole states are split by 10–20 meV, according to both theory and experiment. Since the splitting is small compared with vibrational energies, a model where the core hole is localized to either of the equivalent carbon atoms works well. From accurate ab initio calculations the change in C*–H and C*–C bond distances and C*CH angle following core-ionization are estimated to -5.2 pm (including an empirical correction), -0.4 pm and -2.9° , respectively. A qualitative model based on the concepts of hybridization and valence contractions is able to rationalize these findings.

Acknowledgment. T.K., K.J.B., and L.J.S. gratefully acknowledge The Research Council of Norway for financial support and a grant of computing time (Program for super-computing). T.X.C. and T.D.T. acknowledge support by the National Science Foundation under Grant No. CHE-9727471. E.K., N.B., J.D.B., and the ALS acknowledge support from the Director, Office of Basic Energy Sciences, of the U.S. Depart-

ment of Energy under Contract No. DE-AC03-76SF00098. The experimental work was carried out using the Atomic and Molecular facility funded by DOE, Office of Science, 1996 facility initiative, BES, Chemical Sciences.

Appendix. Computational Procedures

All calculations on ethane were performed in its staggered conformation, leading to D_{3d} symmetry for the neutral state and C_{3v} for the ion with a localized core hole.

Equilibrium geometries, harmonic vibrational frequencies and normal mode vectors are calculated using second-order perturbation theory formulated by Møller and Plesset (MP2),¹² using the Gaussian 94 package.¹³ Using these results, the intensities are obtained within the Franck–Condon principle, as described in ref 6 and implemented in the utility program *g2fc*,²⁷ and further modified according to Malmqvist and Forsberg¹⁵ to take into account the difference in normal modes between the neutral and core-ionized state.

All ab initio calculations were performed employing atom-centered primitive Gaussian-type functions as C: [10s, 5p, 3d] and H: [5s, 2p]. The bases were obtained by decontracting Dunning's cc-pVTZ sets,²⁸ and remove the d and f functions for hydrogen and carbon, respectively. A tight d-function with exponent 3.5 was added to the carbon set.

Two levels of theory have been applied to represent the core-ionized carbon atom. At the lower level, the core of the ionized carbon atom was represented by a modification of the effective core-potential (ECP) by Stevens et al.,²⁹ and this model was used in the MP2 calculations. The ECP is scaled to account for only one electron in the 1s shell as described in ref 7. In the second, more accurate approach, a localized core-hole orbital was explicitly included and variationally optimized as described in ref 7. The latter representation of the core hole was used for a set of geometries calculated at the modified coupled pair functional (MCPF) level of theory³⁰ in a validation of the geometries calculated at the MP2 level of theory. In the MCPF calculations, the geometries were optimized using energy evaluations only.³¹

To validate the quality of the diabatic approximation, the electronic coupling integral between the states where the core-hole is localized at either the *right* or the *left* carbon, was calculated by means of a restricted active space state-interaction (RASSI) calculation³² in a D_{3d} geometry intermediate between the two localized core-hole state geometries. Both the MCPF and RASSI calculations were performed using the MolCas 4.0 suite of programs.³³

Natural bond orbital (NBO) analyses²⁴ were performed using the Gaussian 94 package.¹³ The calculations were performed in the ground-state geometries of C_2H_2 , and C_2H_6 , as obtained in MP2 calculations as described above for ethane. The equivalent-cores approximation was used for the core-ionized molecule, i.e., the core-ionized carbon is represented by N^+ , since the NBO analysis as implemented in Gaussian 94 does not allow for the use of an ECP.

References and Notes

- (1) Köppe, H. M.; Kilcoyne, A. L.; Feldhaus, J.; Bradshaw, A. M. *J. Chin. Chem. Soc.* **1995**, *42*, 255.
- (2) Neeb, M.; Kempgens, B.; Kivimäki, A.; Köppe, H. M.; Maier, K.; Hergenbahn, U.; Piancastelli, M. N.; Bradshaw, A. M. *J. Electron Spectrosc. Relat. Phenom.* **1998**, *88–91*, 19.
- (3) Rennie, E. E.; Köppe, H. M.; Kempgens, B.; Hergenbahn, U.; Kivimäki, A.; Maier, K.; Neeb, M.; Rüdell, A.; Bradshaw, A. M. *J. Phys. B: At. Mol. Opt. Phys.* **1999**, *32*, 2691.
- (4) Kempgens, B.; Köppe, H. M.; Kivimäki, A.; Neeb, M.; Maier, K.; Hergenbahn, U.; Bradshaw, A. M. *Phys. Rev. Lett.* **1997**, *79*, 35.
- (5) Osborne, S. J.; Sundin, S.; Ausmees, A.; Svensson, S.; Sæthre, L. J.; Svaeren, O.; Sorensen, S. L.; Végh, J.; Karvonen, J.; Aksela, S.; Kikas, A. *J. Chem. Phys.* **1997**, *106*, 1661.
- (6) Thomas, T. D.; Sæthre, L. J.; Sorensen, S. L.; Svensson, S. *J. Chem. Phys.* **1998**, *109*, 1041.
- (7) Karlsen, T.; Børve, K. J. *J. Chem. Phys.* **2000**, *112*, 7979.
- (8) Berrah, N.; Langer, B.; Wills, A. A.; Kuk, E.; Bozek, J. D.; Farhat, A.; Gorczyca, T. W. *J. Electron Spectrosc. Relat. Phenom.* **1999**, *101*, 1.
- (9) Myrseth, V.; Bozek, J. D.; Kuk, E.; Sæthre, L. J.; Thomas, T. D. *J. Electron Spectrosc. Relat. Phenom.* **2001**, in press.
- (10) From an isotopic shifts of -30 meV in the difference between zero-point vibrational energies for ground and core-ionized states, as computed at the MP2 level of theory (see Appendix for details).
- (11) Børve, K. J.; Sæthre, L. J.; Thomas, T. D.; Carroll, T. X.; Berrah, N.; Bozek, J. D.; Kuk, E. *Phys. Rev. A* **2001**, *63*, 012506.
- (12) Møller, C.; Plesset, M. S. *Phys. Rev.* **1934**, *46*, 618.
- (13) Frisch, M. J.; Trucks, G. W.; Schlegel, H. B.; Gill, P. M. W.; Johnson, B. G.; Robb, M. A.; Cheeseman, J. R.; Keith, T.; Petersson, G. A.; Montgomery, J. A.; Raghavachari, K.; Al-Laham, M. A.; Zakrzewski, V. G.; Ortiz, J. V.; Foresman, J. B.; Cioslowski, J.; Stefanov, B. B.; Nanayakkara, A.; Challacombe, M.; Peng, C. Y.; Ayala, P. Y.; Chen, W.; Wong, M. W.; Andres, J. L.; Replogle, E. S.; Gomperts, R.; Martin, R. L.; Fox, D. J.; Binkley, J. S.; Defrees, D. J.; Baker, J.; Stewart, J. P.; Head-Gordon, M.; Gonzalez, C.; Pople, J. A. *GAUSSIAN 94*, Revision B.1; Gaussian, Inc.: Pittsburgh, PA, 1995.
- (14) Shimanouchi, T. *Tables of Molecular Vibrational Frequencies Consolidated Volume I*; National Bureau of Standards, 1972; pp 1–160.
- (15) Malmqvist, P.-Å.; Forsberg, N. *Chem. Phys.* **1998**, *228*, 227.
- (16) Kuk, E. *SPANCF 2000* – <http://www.geocities.com/ekuk>.
- (17) van der Straten, P.; Morgenstern, R.; Niehaus, A. *Z. Phys. D.* **1988**, *8*, 35.
- (18) Carroll, T. X.; Berrah, N.; Bozek, J. D.; Hahne, J.; Kuk, E.; Sæthre, L. J.; Thomas, T. D. *Phys. Rev. A* **1999**, *59*, 3386.
- (19) Gray, D. L.; Robiette, A. G. *Mol. Phys.* **1979**, *90*, 1901.
- (20) Karlsen, T.; Børve, K. J. *J. Chem. Phys.* **2000**, *112*, 7986.
- (21) Bevington, P. R. *Data Reduction and Error Analysis for the Physical Sciences*; McGraw-Hill Book Co.: New York, 1969; p 245.
- (22) Sæthre, L. J.; Siggel, M. R.; Thomas, T. D. *J. Electron Spectrosc. Relat. Phenom.* **1989**, *49*, 119.
- (23) Kempgens, B.; Köppel, H.; Kivimäki, A.; Neeb, M.; Cederbaum, L. S.; Bradshaw, A. M. *Phys. Rev. Lett.* **1997**, *79*, 3617.
- (24) Reed, A. E.; Curtiss, L. A.; Weinhold, F. *Chem. Rev.* **1988**, *88*, 899.
- (25) Walsh, A. D. *Discuss. Faraday Soc.* **1947**, *2*, 18.
- (26) McWeeny, R. *Coulson's Valence*, 3rd ed.; Oxford University Press: New York, 1979; p 197.
- (27) Børve, K. J. *g2fc*; University of Bergen, Norway, 1999.
- (28) Dunning, T. H., Jr. *J. Chem. Phys.* **1989**, *90*, 1007.
- (29) Stevens, W. J.; Basch, H.; Krauss, M. *J. Chem. Phys.* **1984**, *81*, 6026.
- (30) Chong, D. P.; Langhoff, S. R. *J. Chem. Phys.* **1986**, *84*, 5606.
- (31) Børve, K. J.; Sierka, M. A.; Todnem, K. *MOLOPT*; University of Bergen, Bergen, Norway, 1995.
- (32) Malmqvist, P.-Å.; Roos, B. O. *Chem. Phys. Lett.* **1989**, *155*, 189.
- (33) Andersson, K.; Blomberg, M. R. A.; Fülcher, M. P.; Karlström, G.; Lindh, R.; Malmqvist, P.-Å.; Neogrády, P.; Olsen, J.; Roos, B. O.; Sadlej, A. J.; Schütz, M.; Seijo, L.; Serrano-Andrés, L.; Siegbahn, P. E. M.; Widmark, P.-O. *MOLCAS 4*; Lund University: Lund, Sweden, 1997.
- (34) *Handbook of Chemistry and Physics*, 76th ed.; Lide, D. R., Ed.; CRC Press: Boca Raton, FL, 1995–96; pp 9–31.